Proactive Operation of Electric Vehicles in Harmonic Polluted Smart Distribution Networks

Sasan Pirouzi[1], Jamshid Aghaei[1], Taher Niknam[1],
Hossein Farahmand[2], and Magnus Korpås[2]

[1]Department of Electrical and Electronics Engineering, Shiraz University of Technology, Shiraz, Iran
[2]Department of Electric Power Engineering, Norwegian University of Science and Technology (NTNU), Trondheim NO-7491, Norway

[*]*Corresponding Author*: **J. Aghaei**, Department of Electronics and Electrical Engineering, Shiraz University of Technology, Shiraz, Iran, phone: +98-912-5865573; fax: +98-71-37353502; e-mail: aghaei@sutech.ac.ir

Abstract— This study proposes combined framework for proactive operation, i.e. bidirectional active and reactive power management, of the smart distribution network as well as harmonic compensation of non-linear loads using electric vehicles (EVs) equipped with bidirectional chargers. The problem is in the form of non-linear programming (NLP) where the objective function is to minimise the voltage deviation at the fundamental frequency and the total harmonic distortion. The harmonic load flow equations, EVs constraints, system operation and harmonic indexes limits are formulated as problem constraints. The proposed NLP problem is converted to an equivalent mixed integer linear programming (MILP) model using Taylor series and linearisation techniques for AC power flow formulation. Also, the Benders decomposition (BD) algorithm is used to solve the proposed MILP problem that is tested on different distribution test networks to demonstrate its efficiency and performance. The results show that the NLP model can be substituted with the high-speed linear programming model. Moreover, the computation speed is improved by using the BD method. Finally, the network and harmonic indexes improved and charging cost reduced using the proposed idea.

Index Terms— Electric Vehicles (EVs), Proactive Operation, Harmonic Compensation, Total Harmonic Distortion (THD), Mixed Integer Linear Programming (MILP), Benders Decomposition (BD).

Nomenclature

1) Indices and Sets:

(b,j), t, h, l, k	Indices of bus, time, harmonic, linearization segments of voltage magnitude term and circular constraint
φ_b, φ_t, φ_h, φ_l, φ_k	Sets of bus, time, harmonic, linearization segments of voltage magnitude term and circular constraint

2) Variables: All variables are in per unit (pu)

ID, IE, IG, IL	Load, parking lot, station and line current
PB, W, QC	Active power and energy of total batteries and reactive power chargers in the parking lot
PE, PG, PL	Parking lot, station and line active power
PE^+, PE^-	Positive and negative part of PE
PLC, QLC	Active and reactive power loss of chargers in the parking lot
QE, QG, QL	Parking lot, station and line reactive power
QE^+, QE^-	Positive and negative part of QE
S, U, I	Apparent power, complex voltage and current
THD^v	Voltage THD without unit
V, ΔV, θ	Magnitude, deviation and angle of voltage
xp, xq	Binary variables in linearization of PE and QE

3) Constants:

A	Bus incidence matrix (if line existed between buses b and j, $A_{b,j}$ is equal to 1,otherwise zero)
ABC, W^0	All battery capacity and initial energy in parking lot in pu
a_r, a_{im}	Coefficients of active power loss of chargers
b_r, b_{im}	Coefficients of reactive power loss of charger
g, b, y	Line conductance, susceptance, admittance in pu
HF	Harmonic factor current without unit
IE^{max}, SE^{max}	Maximum current & power of parking lot in pu
IG^{max}, SG^{max}	Maximum current and power of station in pu
IL^{max}, SL^{max}	Maximum current and power of line in pu
PB^{max}	Charge rate of all batteries in parking lot in pu
PD, QD, SD	Active, reactive and apparent load in pu
T_{step}	Time step in hour
THD^{max}	Maximum voltage THD without unit
TPF	Tangent value in minimum power factor point

V^{max}, V^{min}, V_{ref}	Maximum and minimum voltage and voltage magnitude for reference bus in pu
Y	The network admittance matrix in pu

1 Introduction

The electric vehicles (EVs) are new technology to reduce the environmental pollution and emissions, and also, the main types of EVs such as plug-in hybrid electric vehicles (PHEVs) are connected to the network to provide electrical energy to the batteries. Moreover, the EVs are often connected to the network at the peak load times resulting in high demand of energy at the peak hours, increasing of power losses, voltage drop, congestion of lines and energy cost [2-5]. It is noted that, the EV battery is connected to the network through a charger including AC-DC and DC-DC converters [6]. Generally, the EVs use a unidirectional chargers that tranfer the energy in one direction, i.e., network to battery, and inject the harmonic current to the network [6, 7]. Hence, the network power quality is reduced and the life time of electrical equipments of the network would be degraded or corrupted [7-9].

For decreasing energy demand at the peak hours, several researches have presented the energy management of EVs in the power network [10]-[18]. The authors of [10] and [11] considered the charging management as the EVs energy management using an optimization framework for minimizing network load variation and energy cost. Based on the results of these works, the EVs are charged at low load period and hence, the penetration rate of EVs into network is increased. It is noted that the term of "*penetration rate of EVs*" refers to rate of number of EVs that plugged into network and total EVs that want to connected into network. In this condition, the network operation indices such as voltage of buses could not be improved at the all period, because, EVs only are charged or not discharged in the previous works in the area. Hence, the EVs acts as load. But, the penetration rate of EVs and the network indexes have been improved based on the results of [12]-[18]. In [12]-[14], the EVs energy management strategy refers to charging/discharging management of EVs batteries. [15] and [16] used energy management of EVs as the charging/discharging management of EVs' batteries, and distributed generations (DGs) such as solar and wind systems, and [17] and [18] have presented proactive operation (active and reactive power management) in the distribution network using EVs.

To decrease the harmonic current injection into the network, [19] and [20] have suggested to change the structure of EVs' charger to a bidirectional charger. This charger can control active and reactive power in two sides, i.e., network to charger and charger to network, and can control harmonic current. In these works, the metering point is terminal point of the bidirectional charger, thus, the total harmonic distortion (THD) of the current for the new EVs' charger has been reduced. But, [21] proposes that if EVs are charged by group instead of individually, accordingly the current THD for the group of EVs is less than the current THD for the individual EV. Finally, the problem model of the [10]-[18] is as NLP, and generally, these reference proposed active power management in the network. Also, [19]-[21] considered harmonic compensation of EVs.

Based on the results of [19] and [20], the EVs' bidirectional charger is designed in such a way to control the harmonic current of its terminal while metering point is the charger output point. Accordingly, it compensates only the EVs' current harmonics. However, the EVs' bidirectional charger can control the harmonics of the load current if the load terminal is selected as the metering point. The structure of AC-DC converter in the bidirectional charger like the FACTS devices such as D-STATCOM or STATCOM [22, 23] can control the load harmonic current. Accordingly, this paper presents an optimization approach to consider joint proactive operation of active an reactive power of the smart energy distribution network and harmonic compensation of non-linear loads using EVs bidirectional charger. Hence, the harmonic load (power) flow (HLF) is expressed for the distribution network operation at the first step. Also, the deterministic optimization of the problem is extracted in the form of the non-linear problem with the objective of minimizing the voltage deviation at the fundamental frequency and the voltage THD subject to the HLF equation, system operation limits, EVs and harmonic indexes constraints. While solving the non-linear programming problems is intractable and revealing local optimal solution due to non-linear properties of the problem, therefore, the equivalent mixed integer linear programing (MILP) model of the non-linear problem is expressed in the next step. At the last step, to accelerate the solution speed, the Benders decomposition (BD) is used to solve the MILP problem. In other words, for large scale networks, the calculation time is still a challenge even with linear formulations. To deal with this issue, decomposition approaches such as [24, 25] should be implemented. Therefore, to the best of authors' knowledge, the contributions of this paper with respect to the previous ones are threefold:

- Proactive operation of the active and reactive power and compensating non-linear load harmonic in a distribution network simultaneously using EVs' bidirectional charger.
- Nonlinear modeling of the proactive operation problem of combined active and reactive power management and harmonic compensation using EVs while considering the minimization of the voltage deviation at the fundamental frequency and the voltage THD as objective functions.
- Presenting a tractable equivalent MILP model for the proposed problem to have global optimal solution.
- Using the Benders Decomposition (BD) approach to accelerate the solution of the MILP problem.

Finally, Section 2 describes the harmonic load flow in the distribution network, and Section 3 expresses the original NLP model, MILP model and solution method. Sections 4 and 5 demonstrate numerical simulations and conclusions, respectively.

2 Harmonic load flow

There are different non-linear loads in the distribution networks, hence, the waveform of the network quantities are not sinusoidal. Therefore, the conventional load flow (CLF) cannot be used for the harmonic polluted networks. In this condition, harmonic load flow (HLP) should be implemented to account for fundamental and harmonic frequencies. In the HLF, the apparent power for each bus is represented as follows [26, 27]:

$$S_b = \sum_{h\in\varphi_b} U_b^h \left(I_b^h\right)^* \tag{1}$$

Where, *h* is the harmonic order. Based on the equation (1), two models are considered for HLP [26, 27]:

— HLP model I: the power components are presented only at the fundamental frequency.

— HLP model II: the power components are presented at both the fundamental frequency and harmonic frequencies.

1) *HLP model I:* in this model, the injected apparent power of a bus is calculated by the voltage and injection current of the bus at the fundamental frequency that presented in equation (2) same as the CLF [26-28].

$$S_b = U_b^1 \left(I_b^1\right)^* \tag{2}$$

Note that, this model needs to calculate the injection current according to (3) that is called current flow at the harmonic frequencies [26-28]. In this equation, the network admittance matrix depends on the harmonic frequency, hence, the index of *h* is used in this formula. Therefore, the HLP model I uses the equation (2) same as the CLF, and equation (3).

$$I_b^h = \sum_{j\in\varphi_b} Y_{b,j}^h U_j^h \tag{3}$$

2) *HLP model II:* in this model, the injected apparent power of a bus is calculated by the voltage and injection current of the bus at the fundamental and harmonic frequencies that presented in equation (1) [26, 27]. Also, the equation (3) is used for calculating the injection current and voltage at the harmonic frequencies.

3 Problem formulation

3.1 *The Original Model*

In this section, the proposed deterministic NLP problem model is presented based on Fig. 1. The objective function of this problem is minimization of the voltage deviation at fundamental frequency and voltage THD to investigate EVs' capability to improve the voltage profile, compensate the nonlinear load harmonic and motivate EVs for energy, power and harmonic current control. In the proposed model, the following assumptions are considered:

— While the main aim of this paper is to investigate the capability of EVs equipped with bidirectional chargers for proactive operation and harmonic compensation, hence, the capacitor, distributed generation and other power elements are not considered in the proposed model. However, they are straight forward to be included in the formulation.

— EVs are connected into the distribution network at the parking lot or parking of the apartment after their last trip.

— The HLP model I is used in this paper.

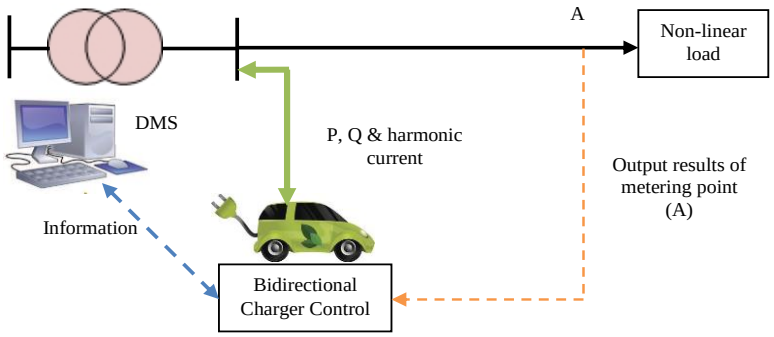

Fig. 1. The structure of EV connection to the network

Therefore, the proposed problem minimises the voltage deviation at fundamental frequency and voltage THD, and it is subjected to the HLP constraints, system operation limits, EVs or parking lot constraints, constraints of harmonic indexes.

1) *Objective function:* the first term of the objective function (4) refers to the voltage deviation, and the voltage THD is expressed in the second part of the objective function. It is noted the dimensions of both terms are the same. Based on the first term, the voltage at the harmonic frequency may be increased however the voltage at the fundamental frequency will be reduced.

$$\min_{V,THD^V} \sum_{b\in\varphi_b} \sum_{t\in\varphi_t} \left\{ \left(\frac{V_{b,t,1} - V_{ref}}{V_{ref}} \right)^2 + THD_{b,t}^V \right\} \tag{4}$$

2) *The HLP constraints:* these constraints are presented in the equations (5) to (12). Constraints (5) to (9) indicate the load flow equations that include active power balance (5), reactive power balance (6), active and reactive power flow of lines (7) and (8), and the value of the voltage angle in the reference bus (9) [29]. Equation (10) and (11) present the relationship between the injection current, i.e., *IG*, *IE*, *ID*, and voltage at the harmonic frequency [26]. Equation (12) expresses that the harmonic current of the load is the pre-determined percentage of the load apparent power. Also, *PG*, *QG* and *IG* in the network buses except the substation bus are equal to zero based on the first assumption.

$$PG_{b,t} - PE_{b,t} - \sum_{j \in \varphi_b} A_{b,j} PL_{b,j,t} = PD_{b,t} \quad \forall\, b, t \tag{5}$$

$$QG_{b,t} - QE_{b,t} - \sum_{j \in \varphi_b} A_{b,j} QL_{b,j,t} = QD_{b,t} \quad \forall\, b, t \tag{6}$$

$$PL_{b,j,t} = g_{b,j,1}(V_{b,t,1})^2 - V_{b,t,1}V_{j,t,1}\begin{Bmatrix} g_{b,j,1}\cos(\theta_{b,t} - \theta_{j,t}) \\ +b_{b,j,1}\sin(\theta_{b,t} - \theta_{j,t}) \end{Bmatrix} \quad \forall b, j, t \tag{7}$$

$$QL_{b,j,t} = -b_{b,j,1}(V_{b,t,1})^2 + V_{b,t,1}V_{j,t,1}\begin{Bmatrix} b_{b,j,1}\cos(\theta_{b,t} - \theta_{j,t}) \\ -g_{b,j,1}\sin(\theta_{b,t} - \theta_{j,t}) \end{Bmatrix} \quad \forall b, j, t \tag{8}$$

$$\theta_{b,t} = 0 \quad \forall\, b = reference\,bus, t \tag{9}$$

$$IG_{b,t,h} - IE_{b,t,h} - ID_{b,t,h} = \sum_{j \in \varphi_b} A_{b,j} IL_{b,j,t,h} \quad \forall\, b, t, h \neq 1 \tag{10}$$

$$IL_{b,j,t,h} = y_{b,j,h}\left(V_{b,t,h} - V_{j,t,h}\right) \quad \forall\, b, j, t, h \neq 1 \tag{11}$$

$$ID_{b,t,h} = HF_{b,h} SD_{b,t} \quad \forall\, b, t, h \neq 1 \tag{12}$$

3) *System operation limits:* constraints (13) to (16) indicate the system operation limits that include voltage bus, line power flow, station power and equivalent station power factor limits [29]. Note that the distortion power in the lines and stations are not considered in the equations (14) and (15), respectively. Because, the distortion power depends to the voltage and current at the harmonic frequency, hence, the value of this power is less than the main active and reactive powers. Therefore, this power has been ignored in these equations. Also, the equation (16) shows the equivalent station power factor, that *TPF* is equal to the *tan* (*arcos* (minimum power factor)), while the minimum power factor is considered 0.9.

$$V^{\min} \le V_{b,t,1} \le V^{\max} \quad \forall\, b, t \tag{13}$$

$$(PL_{b,j,t})^2 + (QL_{b,j,t})^2 \le (SL_{b,j}^{\max})^2 \quad \forall\, b, j, t \tag{14}$$

$$(PG_{b,t})^2 + (QG_{b,t})^2 \le (SG_{b}^{\max})^2 \quad \forall\, b, t \tag{15}$$

$$TPF \times PG_{b,t} \le QG_{b,t} \le TPF \times PG_{b,t} \quad \forall\, b, t \tag{16}$$

4) *EVs or parking lot constraints:* these constraints are introduced in (17) to (27) that indicate the active power balance between network and all EVs' batteries in the parking lot, (17), reactive power balance between network and all EVs chargers in the parking lot, (18), active and reactive power losses of all EVs chargers in the parking lot, (19) and (20), energy of all EVs batteries in the parking lot, (21) to (23), energy, (24), charge/discharge rate, (25), charger capacity, (26), and harmonic current, (27), limits of all EVs in the parking lot [22]. In fact, the active power loss equation of the charger for charging and discharging modes is not the same [30], but, this difference is negligible. Hence, in this paper, the same equation is considered for active power loss of the charging and discharging modes. Also, in equations (21) to (23), W^0 indicates the initial energy of all EVs that connected to the network in the parking lot at hour t (NEV_t). Initial energy of the EV's battery (IEEVB) is equal to $SOC \times BC$ that *SOC* and *BC* are the state of charge and battery capacity, respectively [2]. The *SOC* introduces the percentage of the remained energy in the EV battery, and this term depends to the driving distance of the EV in the electric mode (*L*). Hence, the *SOC* is expressed as $(1 - L/AER)$, where all electrical range (*AER*), presents the total distance that EV derives in the electric mode based on its battery capacity [2]. Therefore, W^0 at the hour t is formulated as $W_t^0 = \sum_{i=1}^{NEV_t} IEEVB_i$. In addition, the parameter of *ABC* is equal to the summation of all EVs battery capacity in the parking lot.

$$PE_{b,t} = PB_{b,t} + PLC_{b,t} \quad \forall\, b, t \tag{17}$$

$$QE_{b,t} = QC_{b,t} + QLC_{b,t} \quad \forall\, b, t \tag{18}$$

$$PLC_{b,t} = a_r \left|PE_{b,t}\right| + a_{im} \left|QE_{b,t}\right| \quad \forall\, b, t \tag{19}$$

$$QLC_{b,t} = b_r \left|PE_{b,t}\right| + b_{im} \left|QE_{b,t}\right| \quad \forall\, b, t \tag{20}$$

$$W_{b,t} = W_{b,t}^0 + T_{step} PB_{b,t} \quad \forall\, b, t = 1 \tag{21}$$

$$W_{b,t} = W_{b,t-1} + W_{b,t}^{0} + T_{step} PB_{b,t} \quad \forall b, t \neq 1 \tag{22}$$

$$W_{b,t} = ABC_b \quad \forall b, t = 24 \tag{23}$$

$$W_{b,t} \geq 0 \tag{24}$$

$$-PB_{b,t}^{\max} \leq PB_{b,t} \leq PB_{b,t}^{\max} \quad \forall b, t \tag{25}$$

$$(PE_{b,t})^2 + (QE_{b,t})^2 \leq (SE_{b,t}^{\max})^2 \quad \forall b, t \tag{26}$$

$$-IE_{b,t,h}^{\max} \leq IE_{b,t,h} \leq IE_{b,t,h}^{\max} \quad \forall b, t, h \tag{27}$$

5) *Constraints of harmonic indexes:* equations (28) to (31) introduce the harmonic index constraints that include voltage THD equation [31], voltage THD limit that is 5% based on IEEE 519 standard [32], the station current limit and the line current limit at the harmonic frequency.

$$THD_{b,t}^{v} = \sqrt{\frac{\sum_{h \in \varphi_h, h \neq 1} \left(V_{b,t,h}\right)^2}{\left(V_{b,t,1}\right)^2}} \quad \forall b, t \tag{28}$$

$$THD_{b,t}^{v} \leq THD_{b}^{\max} \quad \forall b, t \tag{29}$$

$$-IG_{b,h}^{\max} \leq IG_{b,t,h} \leq IG_{b,h}^{\max} \quad \forall b, t, h \tag{30}$$

$$-IL_{b,j,h}^{\max} \leq IL_{b,j,t,h} \leq IL_{b,j,h}^{\max} \quad \forall b, j, t, h \tag{31}$$

3.2 *The MILP Model*

The proposed problem presented in previous subsection is as NLP model duo to non-linear equations of (4), (7), (8), (19), (20) and (28), and circular inequality (14), (15) and (26). Also, NLP problems are intrinsically more difficult to solve with respect to linear problems, and there is no guarantee to reach optimal solution [29]. Hence, in this paper, a MILP model is proposed to the original NLP problem as follows:

1) *Linear approximation to HLP equations:* constraints (7) and (8) in the HLP model are non-linear equations. For linear approximation of these constraints, this paper considers the following assumptions [29]:

— The difference of voltage angle between two buses (across a line) is less than 0.105 radian.

— The voltage magnitude at the fundamental frequency can be written as $V^{\min} + \sum_{l \in \varphi_l} \Delta V_l$ based on the piecewise linearization method [33] and Fig. 2, wherein $\Delta V << 1$.

It is expressed that the difference of voltage angle across a line is less than 0.105 radian based on power flow results of different distribution networks [34-36] that is shown in table 1. Therefore, based on the first assumption, **sin** (θ_b-θ_j) and **cos** (θ_b-θ_j) are equal to (θ_b-θ_j) and 1, respectively. Also, based on the second assumption, V^2 and V_bV_j are respectively equal to:

$$V^2 = \left(V^{\min}\right)^2 + \sum_{l \in \varphi_l} m_l \Delta V_l \tag{32}$$

$$V_b V_j = \left(V^{\min}\right)^2 + V^{\min} \sum_{l \in \varphi_l} \Delta V_{b,l} + V^{\min} \sum_{l \in \varphi_l} \Delta V_{j,l} \tag{33}$$

where m is the line slope. It is noted that ΔV^2, $\Delta V \times (\theta_b$-$\theta_j)$ and $(\theta_b$-$\theta_j)^2$ are negligible, and these terms are considered to be zero in this paper. Therefore, the linear approximation of equations (7) and (8) are as follows:

Table 1: Maximum difference of voltage angle across a line.

Network	33-Bus	69-Bus	123-Bus
Maximum value of (θ_i-θ_j)	-0.004	-0.006	-0.009

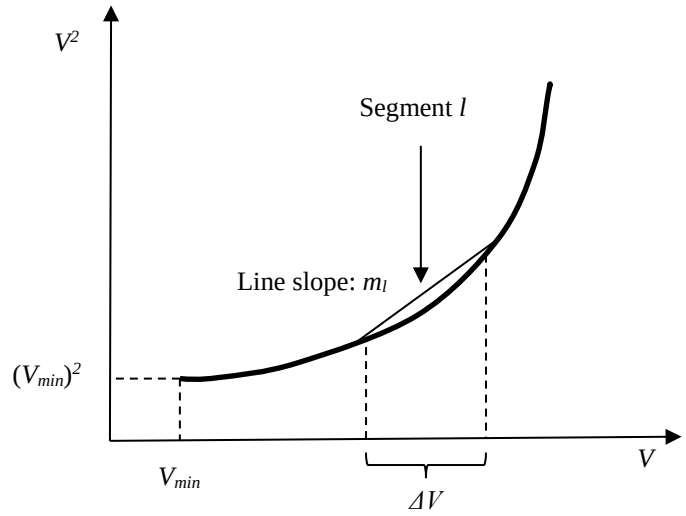

Fig. 2. The piecewise linearization method [33]

$$PL_{b,j,t} = g_{b,j,1}\left(\sum_{l\in\varphi_i}\left(m_l - V^{\min}\right)\Delta V_{b,t,1,l} - V^{\min}\Delta V_{j,t,1,l}\right) - \left(V^{\min}\right)^2 b_{b,j,1}(\theta_{b,t}-\theta_{j,t}) \quad \forall b,j,t \tag{34}$$

$$QL_{b,j,t} = -b_{b,j,1}\left(\sum_{l\in\varphi_i}\left(m_l - V^{\min}\right)\Delta V_{b,t,1,l} - V^{\min}\Delta V_{j,t,1,l}\right) - \left(V^{\min}\right)^2 g_{b,j,1}(\theta_{b,t}-\theta_{j,t}) \quad \forall b,j,t \tag{35}$$

2) *Linear approximation of system operation limits:* constraint (13) is written as follows based on the second assumption of the previous subsection:

$$\Delta V_{b,t,l} \le \Delta V^{\max} \quad \forall\, b,t,l \tag{36}$$

where ΔV is positive variable based on Fig. 2, and ΔV^{max} is equal to $(V^{max}\text{-}V^{min})/N_l$, where N_l is the number of linearization segments of the voltage magnitude term. Constraints (14) and (15) are as circular inequality. Based on idea in Fig. 3, the linear approximation equations of these constraints are written as follows:

$$\cos(k\Delta\alpha)\times PL_{b,j,t} + \cos(k\Delta\alpha)\times QL_{b,j,t} \le SL_{b,j}^{\max} \quad \forall\, b,j,t,k \tag{37}$$

$$\cos(k\Delta\alpha)\times PG_{b,t} + \cos(k\Delta\alpha)\times QG_{b,t} \le SG_{b}^{\max} \quad \forall\, b,t,k \tag{38}$$

Based on the above equations, the circular constraint is approximated by a polygon. Each edge of the polygon is a straight line and their equations are obtained from the tangents to the circle at different points as shown in Fig. 3 [37]. In other words, these equations linearized based on Fig. 3, but it is noted that in the case of a small number of piece-wise linear sections, the error value in this method would be high. Therefore, the number of piece-wise linear sections with different angles from horizontal axis should be increased to reduce the linearization error. Hence, the 360 degrees of circle perimeter are divided into equal parts $\Delta\alpha$. Then, the line equation is linearized for each $k\Delta\alpha$, where k is the linearization segments index. Finally, the calculated line equation is integrated into a circle with a radius less than or equal to S.

$k=\{1, \ldots, n_k = 6\}$, $\Delta\alpha=2\pi/n_k=\pi/3$

Second tangent line (k=2), the line equation is:

$$\cos(2\times\frac{\pi}{3})P+\sin(2\times\frac{\pi}{3})Q=S^{\max}$$

$$\Rightarrow -\frac{1}{2}P+\frac{\sqrt{3}}{2}Q=S^{\max}$$

And second feasible region:

$$-\frac{1}{2}P+\frac{\sqrt{3}}{2}Q\le S^{\max}$$

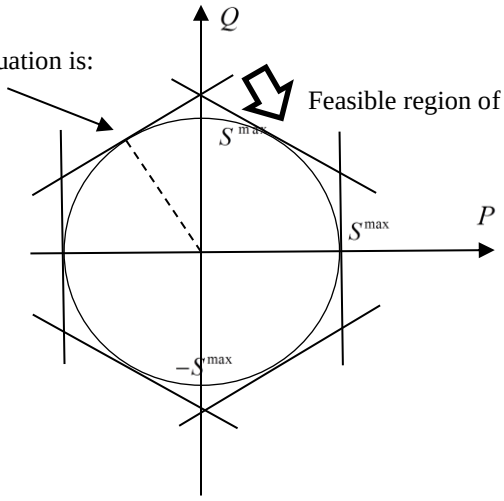

Fig. 3. Linearization of circular constraint.

3) *Linear approximation to parking lot constraints:* constraints (19) and (20) in the EVs or parking lot constraints, are non-linear equations due to the absolute terms of $|PE|$ and $|QE|$. For linearization, PE and QE are converted to two positive ($\ge$0) and negative ($\le$0) parts. Therefore, the absolute terms of $|PE|$ or $|QE|$ can be written as (PE^+ - PE^-) or (QE^+ - QE^-), while PE^+, PE^-, QE^+ and QE^- have been positive value. Hence, the constraints (19) and (20) are substituted by the following equations:

$$PLC_{b,t}=a_r\left(PE^+_{b,t}-PE^-_{b,t}\right)+a_{im}\left(QE^+_{b,t}-QE^-_{b,t}\right)\ \forall b,t \tag{39}$$

$$QLC_{b,t}=b_r\left(PE^+_{b,t}-PE^-_{b,t}\right)+b_{im}\left(QE^+_{b,t}-QE^-_{b,t}\right)\ \forall b,t \tag{40}$$

$$PE_{b,t}=PE^+_{b,t}+PE^-_{b,t}\ \forall b,t \tag{41}$$

$$QE_{b,t}=QE^+_{b,t}+QE^-_{b,t}\ \forall b,t \tag{42}$$

$$PE^+_{b,t}\le SE^{\max}_{b,t}xp_{b,t}\ \forall b,t \tag{43}$$

$$-SE^{\max}_{b,t}(1-xp_{b,t})\le PE^-_{b,t}\ \forall b,t \tag{44}$$

$$QE^+_{b,t}\le SE^{\max}_{b,t}xq_{b,t}\ \forall b,t \tag{45}$$

$$-SE^{\max}_{b,t}(1-xq_{b,t})\le QE^-_{b,t}\ \forall b,t \tag{46}$$

It is noted that if PE^+ (QE^+) $\neq$ 0, PE^- (QE^-) is equal to zero. Thus, the equations (43)-(46) used in the linearization equations of (19) and (20). In addition, the constraint (26) is as circular inequality that is converted to the linear constraint as follows:

$$\cos(k\Delta\alpha)PE_{b,t}+\cos(k\Delta\alpha)QE_{b,t}\le SE^{\max}_{b,t}\quad\forall b,t,k \tag{47}$$

4) *Linear approximation of harmonic index constraints:* constraint (28) is a non-linear equation. For linearization, the following constraints are used as an equivalent equation of (28) and (29):

$$V_{b,t,h}\le V^{\max}_{b,h}\quad\forall b,t,h\neq 1 \tag{48}$$

Where, $V^{\max}_{b,h}$ is 3% of $V_{b,t,1}$ based on IEEE 519 standard [32]. It should be noted that $V_{b,t,h}$ is a positive variable.

5) *Linear approximation of objective function:* for linearization of the first part of the objective function (voltage deviation), the term of $(V-V_{ref})^2$ is converted to $(V^2-2V_{ref}V+V_{ref}^2)$ in the first step. In the next step, the first part of the objective function is rewritten as the following linear equation based on the second assumption of section 3.2-1:

First part of the objective function

$$=\sum_{b\in\varphi_b}\sum_{t\in\varphi_t}\frac{\left(V_{ref}-V^{\min}\right)^2+\sum_{l\in\varphi_l}\left(m_l-2V_{ref}\right)\Delta V_{b,t,1}}{V_{ref}{}^2} \tag{49}$$

Furthermore, the second part of the objective function is changed to the following linear equation based on the equivalent equation of section 3.2-4:

$$Second\ part\ of\ the\ objective\ function = \sum_{b\in\varphi_b}\sum_{t\in\varphi_t}\sum_{h\in\varphi_h}\frac{V_{b,t,h}}{V_{ref}} \tag{50}$$

Therefore, the MILP model of the original problem is written as follows:

$$\min_{\Delta V,V} \quad Eq(49)+Eq(50) \tag{51}$$

Subject to:

(5), (6), (9)-(12), (16)-(18), (21)-(25), (27), (30), (31), (34)-(46) (52)

3.3 *Solution Method*

Due to the presence of the complicating constraints, i.e., (36)-(38), to accelerate the optimization problem, the BD algorithm is used [38]. The base problem, i.e., (51) and (52) without (36)-(38) solved in the master problem. Then the system operation limits, i.e., (36)-(38), are checked based on the output results of the master problem. This step is called the sub-problem and its model presented as follows:

$$\min_{S} \quad F_{sp}=\sum S \tag{53}$$

Subject to:

$$Left\ side\ of\ Eq(36)_{b,t,l}-S_{b,t,l,1}\le \Delta V^{\max}:\pi_{b,t,l,1} \quad \forall\, b,t,l \tag{54}$$

$$Left\ side\ of\ Eq(37)_{b,j,t,k}-S_{b,j,t,k,2}\le SL_{b,j}^{\max}:\pi_{b,j,t,k,2} \ \forall\, b,j,t,k \tag{55}$$

$$Left\ side\ of\ Eq(38)_{b,t,k}-S_{b,t,k,3}\le SG_{b}^{\max}:\pi_{b,t,k,3} \quad \forall\, b,t,k \tag{56}$$

In the above problem, S ($\ge$0) and π are the slack and dual variables, respectively. In this algorithm, if the proposed problem has not converged ($|F_{sp}|\ge\varepsilon$, which ε is BD convergence tolerance), the Benders cut is added to the master problem which is reformulated as (55) [38]. This process is continued until the problem is converged ($|F_{sp}|\le\varepsilon$). The flowchart of implementing BD for the proposed problem is shown in Fig. 4.

$$\sum_{i=(36)-(38)}\sum \pi_i\times(right\ side-left\ side)\ of\ Eq(i)\le 0 \tag{57}$$

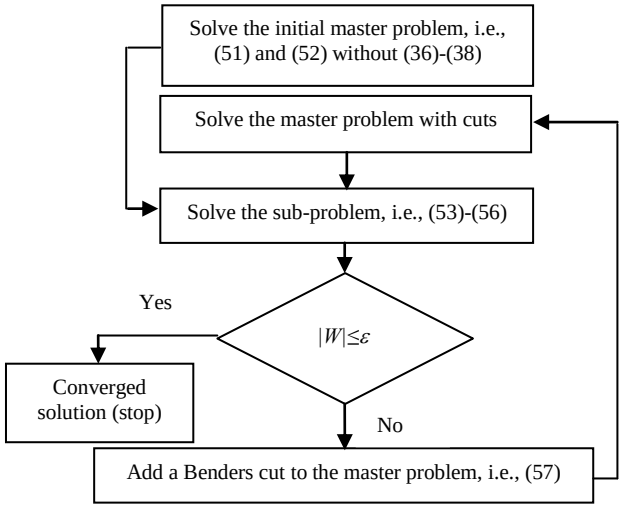

Fig. 4. BD algorithm to solve proposed problem.

4 Numerical results and discussion

4.1 *Case Study Data*

The radial 33-bus distribution network is used as the test network that its characterization such as line, load and etc presented in [34]. The time interval or T_{step} is one hour, and the start time for the simulation studies is 10:00 A.M due to equations (21)-(24). These equations in hour t depend on hour $t-1$. The loads data at the peak load time is based on [34], and loads at non-peak times are obtained by using multiplying loads in peak load condition and load percent curve, shown in Fig. 5. The maximum and minimum voltages are 1.05 and 0.9 per unit, respectively, and the voltage magnitude for reference bus (bus 1) is equal to 1 per unit. The non-liner load is 6-pulse converter that is plugged to the network in buses of 4, 7, 10, 13, 18, 21, 25, 27, and 30. Harmonic factor current (*HF*) is presented in Table 2. Three groups of EVs' number are considered in the parking lot, and each bus has a parking lot. Indeed, the EVs' number is 21, 30, 60 if the range of active load in per unit is (0, 0.1), (0.1, 0.2) and (0.2,

>0.2), respectively. Also, EV characteristics are presented in Table 3. In (39) and (40), the a_r, a_{im}, b_r and b_{im} are same for all EVs and are equal to 0.09, 0.0475, 0.02 and 0.02, respectively. Also, the IE^{max} is considered to 10% of SE^{max} and 5% SE^{max} for $2 \le h \le 20$ and $h \ge 21$, respectively. Moreover, IL^{max} and IG^{max} is considered 4%, 2%, 1.5%, 0.6% and 0.3% of maximum power of line and station for $h < 11$, $11 \le h < 17$, $17 \le h < 23$, $23 \le h < 35$ and $h \ge 35$, respectively based on standard of IEEE STD. P519.1/D9A [39]. Noted that since the voltage of bus 18 in a 33-bus network is less than other buses based on [34], therefore the bus 18 has been selected for the investigation of the network voltage in this paper.

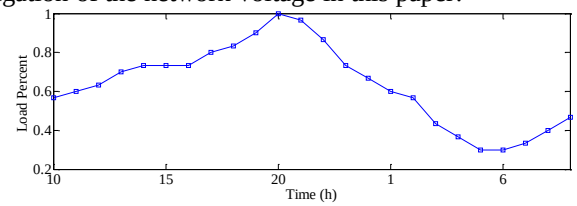

Fig. 5. Daily load percent curve [2].

Table 2: The value of harmonic factor current [34].

H	1	5	7	11	13	17	19
HF^p	1	0.2	0.143	0.091	0.077	0.059	0.053
H	23	25	29	35	37	41	43
HF^p	0.043	0.04	0.034	0.029	0.027	0.024	0.015

Table 3: Characteristics of EV.

Battery capacity (KWh) [6]	BC≤8	8≤BC≤15	BC≥15
State of charge [2]	0	0.15	0.25
Charger capacity (kVA) [6]	3.3	4.6	6.6
Charging time (h) [6]	≤4	2-4	≥2.5
Charge rate (kW) [6]	2	4	6
EVs in each group (%) [2]	20	60	20

4.2 *Results*

In this paper, the GAMS 23.5.2 software and CPLEX solver is used for programming of the proposed problem model [40].

1) *Comparison of MILP and NLP Models*: For this case study, the number of the linearization segments of the voltage magnitude term and circular constraint is 4 and 180, respectively. Table 4 shows the results of this study without BD. As results show, the deviation percent of the network active and reactive power is about 3% for two models. But, this term is about 0.1% and 0.5% for the voltage magnitude and voltage angle, respectively. Thus, the deviation value of the variables is negligible, and the calculation time of the MILP model is less than that of the NLP model. As a result, the performance of the proposed MILP model is satisfactory.

Table 4: Comparison of MILP and NLP deterministic models.

Model	NLP	MILP	Deviation percent
Calculation time (s)	981	227	76.9%
Total active power of the station at 24 hours (pu)	73.24	71.05	2.97%
Total station reactive power at 24 hours (pu)	-16.8	-17.3	-2.94%
Mean of voltage of bus 18 (pu)	0.966	0.965	0.11%
Mean of angle of bus 18 (rad)	-0.054	-0.0543	-0.55%

2) *Studying the performance of BD algorithm*: in this section, two cases are considered: the MILP problem without and with BD algorithm. Also, three distribution networks, i.e., 33-bus, 69-bus [35] and 123-bus [36], are used for this comparison. The data of the non-linear loads (6-pulse converter) are presented in table 5. Also, the other data of the problem for the three distribution networks is same. The results of this section are presented in table 6 that shows the calculation time of two cases and BD accuracy of the case with BD, i.e., the objective function value of the sub-problem $|F_{sp}|$. Based on this table, the calculation time of the proposed MILP problem solution with BD algorithm is less than the calculation time of the case without BD. In addition, the BD convergence value for the proposed problem is low that is acceptable based on the speed calculation of BD algorithm.

Table 5: Data of non-linear loads.

Network	The buses with non-linear load connection
33-bus	4, 7, 10, 13, 18, 21, 25, 27, 30, 33
69-bus	4, 10, 16, 22, 27, 30, 35, 40, 46, 50, 55, 60, 65

123-bus	4, 6, 11, 12, 16, 20, 24, 29, 33, 39, 46, 59, 83, 90, 104

Table 6: Results of implementing BD algorithm.

Network (bus)		33	69	123
Calculation time of (s)	Without BD	227	567	891
	With BD	103	211	301
BD accuracy ($\|F_{sp}\|$ in pu)		0.03	0.10	0.15

3) *Investigating harmonic and network indices*: there are three cases for this study. Indeed, case I investigates the results of the base load (network without EVs) and case II refers to the proposed problem without active power discharge management of EVs while case III refers to the proposed problem with active power discharge management of EVs. The results of this section are shown in Figs. 6 to 9 and table 7. Based on Fig. 6, the EVs are charged at the period of 22:00-9:00 of the next day, and they inject the reactive power to the network at the period of 12:00-9:00 of the next day. Also, EVs are not connected to the network at the period of 10:00-11:00 in the case II. This can be inferred from this fact that as seen in Fig. 6(a), the apparent power of all cases is the same in this period. At the periods of 12:00-21:00 and 8:00-9:00, the injected reactive power of EVs is less than $2\times\Sigma QD$, thus, the network apparent power of case II is less than the case I. But, the network apparent power of the case I is less than the case II at the 22:00-7:00, because, the EVs are charged and the injected reactive power of EVs is greater than $2\times\Sigma QD$ at this period. Noted that the results of the proactive operation for the case III is similar to the case II based on Fig. 6, but the EVs are charged at the period of 12:00-18:00, and the EVs are discharged at the period of 19:00-21:00. Also, the injected reactive power of EVs is less than the case II at these periods. Because of the fact that the absolute active power of EVs is increased in the case III with respect to the case II, hence, the injected reactive power of EVs is reduced based on the constraint (26) or (47) in the case III.

Finally, the network apparent power is increased at 12:00-18:00 and decreased at 19:00-21:00 in the case III with respect to the case II. Furthermore, Fig. 7 shows the voltage results for three cases. Based on Fig. 7(a), the improvement of voltage profile at the peak load time for cases I, II and III are relatively low, medium and high, respectively. Because, the injected active and reactive power of EVs at this time is equal to (PE^{-}, QE^{-}) = (0, 0), (0, not zero) and (not zero, not zero) for cases I, II and III, respectively. In addition, the voltage of all buses has been improved all the times using EVs' proactive operation. For instance, this matter has been shown for bus 18 in Fig. 7(b).

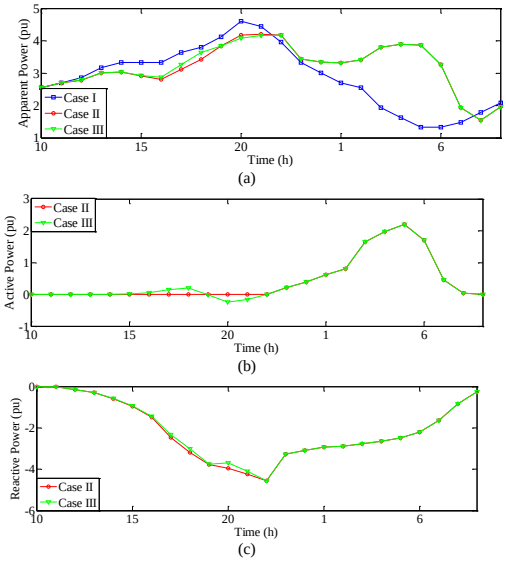

Fig. 6. Daily pattern of (a) the network apparent power, (b) the active power of all EVs, (c) the reactive power of all EVs.

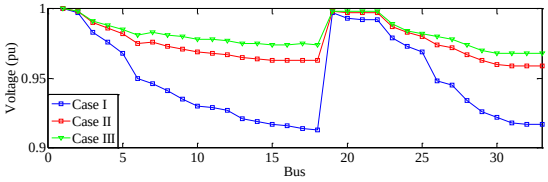

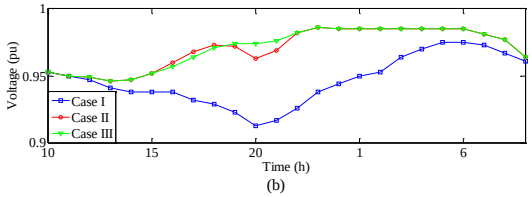

Fig. 7. (a), the voltage profile at the peak load time, (b) daily pattern of the voltage in bus 18.

The daily pattern of the network power factor is shown Fig. 8. Based on this figure, due to implementing the proposed proactive operation mechanism in cases II and III, the network power factor has been improved with respect to the minimum acceptable power factor of 0.9 at the period of 14:00 to 9:00 of the next day in these cases.

The penetration rate of EVs is low at 10:00-13:00, therefore, the network power factor is less than 0.9. Based on this statement, the constraint (16) is expressed at 14:00-9:00. In addition, the voltage THD as a harmonic index has been shown in Fig. 9. Based on the voltage THD profile at the peak load time as depicted in Fig. 9(a), the combined mechanism of the proactive operation and harmonic compensation caused that the voltage THD to be reduced. The decreasing of the voltage THD in the case III is high with respect to the other cases at this time. Because, the voltage of the fundamental frequency in the case III is greater than other cases based on Fig. 7(a), but the voltage of harmonic frequency of case III is the same as case II. Therefore, it can be inferred that the discharging power management is effective for improvement of voltage THD. It is worthy to note that while the compensation strategy of the EVs is set to the main frequency according to HLP model I then it cannot improve the voltage of the harmonic frequency.

However, the voltage THD of all buses has been improved all the times using combined proactive operation and harmonic compensation of EVs as seen in Fig. 9(b).

Table 7 presents the values of the network and harmonic indexes. Based on the results, the energy management and harmonic compensation improves the mean voltage of the network and the voltage THD. But, the energy and equivalent reactive energy losses of this problem have been increased with respect to the base load case. The reason is that during the charging of EVs the drawn extra power from the network-side will increase the network losses. Also, the results of the case II are close to the results of the case III based on Figs. 6-9 and table 7.

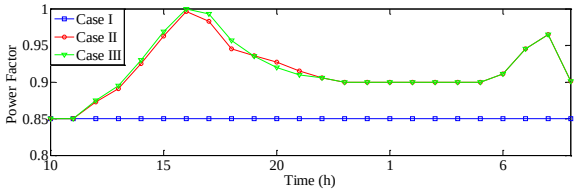

Fig. 8. The daily pattern of the network power factor.

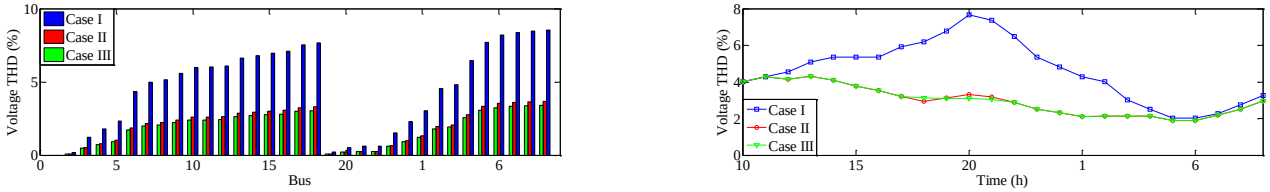

Fig. 9. (a), the voltage THD profile at the peak load time, (b) daily pattern of the voltage THD in bus 18.

Table 7: Simulation results for different cases.

Cases	I	II	III
Mean of voltage at peak load time (pu)	0.9486	0.9754	0.9815
Mean voltage THD at peak load time (%)	4.6186	1.9915	1.8352
Energy loss (pu)	2.0770	2.6490	2.7420
Total reactive power loss at 24 hours (pu)	1.3820	1.7810	1.7960
Charging cost ($)		254.7	264.3
Revenue of discharging power ($)		0	28.8
Revenue of reactive power ($)		111.6	103.3
Revenue due to reducing of voltage THD ($)		43.2	43.2
Total revenue ($)		154.8	175.3
Ratio of revenue/cost (%)		60.78	66.33

4) *Investigating the economy of EVs*: this section studies the cases II and III of the previous subsection. The EVs' cost is charging cost that is equal to $\sum \lambda_t PE^{+}_{b,t}$, where λ_t is the electric energy price in \$/MWh. For this study λ_t is equal to 16 \$/MWh at the period of 1:00 to 7:00, 24 \$/MWh at the periods of 8:00-17:00 and 23:00-24:00, and 30 \$/MWh at the period 18:00 to 22:00 [11]. The revenues of EVs come from the following terms: discharging power ($\sum \lambda_t \left| PE^{-}_{b,t} \right|$), reactive power injection and consumption ($\sum k_1 \lambda_t \left| QE_{b,t} \right|$) and reduced voltage THD. To calculate the revenue of the reduced voltage THD, the following strategy is considered. Indeed, to compensate the harmonics of the load current, the EVs are needed to inject or absorb the current harmonics of loads in such a way to decrease voltage harmonics. For this purpose, EVs will inject or absorb the harmonic components of the load. Therefore, to account for the EVs' revenue of the voltage THD reduction, the harmonic components of the EVs' current should be considered. Accordingly, the last term can be modeled by $\sum k_2 \lambda_t \sqrt{\sum_{h\neq 1} \left(IE_{b,t,h}\right)^2}$, wherein $\sqrt{\sum_{h\neq 1} \left(IE_{b,t,h}\right)^2}$ introduces the effective value of the current of parking lot at the harmonic frequency. Also, $k_1\lambda$ and $k_2\lambda$ are reactive power price (in \$/MVArh) and harmonic current price (in \$/MAh), respectively. Based on [29], the same values are considered for k_1 and k_2 which are equal to 0.08. Consequently, the results of this section are shown in table 7. Based on the results of table 7 and Fig. 6(b), while some of EVs are charged at the period of 12:00-18:00 for case III, the charging cost of case III is greater than the case II. In addition, the EVs revenue due to reactive power in case III is less than the case II. Because, in case III, the EVs inject the active power to the network at the period of 18:00-22:00, thus, according to the constraint (47), SE^{max} do not allow the EVs to inject more reactive power to the network. But in the case II, while the active power discharging mode of EVs is not considered, therefore, the EVs can inject more reactive power in the period of 12:00-21:00 with respect to the case III which results in more revenue from the reactive power for case II. Noted that the revenues of EVs for reducing voltage THD are the same for both cases. All in all, the ratio of revenue/cost is approximately close to each other for both cases. The main reason is that the cost increase for charging EVs and revenue decrease for reactive power support are compensated by the revenue increase due to discharging active power to the network.

5 Conclusions

In this paper, the proactive operation of active and reactive power in smart energy distribution networks and harmonic compensation of non-linear loads using EVs with bidirectional chargers have been presented. The proposed problem minimized the voltage deviation at the fundamental frequency and the voltage THD subject to the harmonic load flow equations, system operation limits, harmonic index equations and EVs constraints. This problem is in the form of NLP, hence, the equivalent MILP model of the original NLP model has been proposed. Finally, the BD algorithm is used for solving the proposed MILP problem to accelerate its computation speed. Based on the results, the network and harmonic indexes have been improved at all the times if charging/discharging and reactive power management and harmonic compensation have been implemented. In addition, in the case of discarding the discharging mode of active power of EVs, the improvement of network and harmonic indexes is approximately similar to the case of considering discharging mode of active power. Also, the ratio of revenue to cost of EVs is close in both cases. Hence, it can be inferred that it is better to ignore discharging active power capability of EVs to prevent decreasing of its battery life. Finally, the research work is underway to consider the uncertain behavior of EVs in the proposed power management of the distribution networks in the presence of EVs.

References

[1] Y. Nie, M. Ghamami, A. Zockaie, F. Xiao, "Optimization of incentive polices for plug-in electric vehicles," *Transportation Research Part B: Methodological*, vol. 84, pp. 103-123, Feb. 2016

[2] L. Zhang, F. Jabbari, T. Brown, S. Samuelsen, "Coordinating plug-in electric vehicle charging with electric grid: Valley filling and target load following," *Journal of Power Sources*, vol. 267, pp. 584-597, Dec. 2014

[3] X. Wu, X. Hu, S. Moura, X. Yin, V. Pickert, "Stochastic control of smart home energy management with plug-in electric vehicle battery energy storage and photovoltaic array," *Journal of Power Sources*, vol. 333, pp. 203-212, November 2016.

[4] S. Habib, M. Kamran, U. Rashid, "Impact analysis of vehicle-to-grid technology and charging strategies of electric vehicles on distribution networks – A review," *Journal of Power Sources*, vol. 277, pp. 205-214, March 2015

[5] E. Talebizadeh, M. Rashidinejad, A. Abdollahi, "Evaluation of plug-in electric vehicles impact on cost-based unit commitment," *Journal of Power Sources*, vol. 248, pp. 545-552, Feb. 2014.

[6] F. He, Y. Yin, S. Lawphongpanich, "Network equilibrium models with battery electric vehicles," *Transportation Research Part B: Methodological*, vol. 67, pp. 306-319, Sept. 2014

[7] C. Jiang, R. Torquato, D. Salles, and W. Xu, "Method to assess the power quality impact of plug- in hybrid electric vehicles," *Power Delivery*, *IEEE Transactions on,* vol. 29, pp. 958- 965, 2014.

[8] S. Pelletier, O. Jabali, G. Laporte, M. Veneroni, "Battery degradation and behaviour for electric vehicles: Review and numerical analyses of several models," *Transportation Research Part B: Methodological*, In Press, Available online 1 March 2017.

[9] A. Montoya, C. Guéret, J. E. Mendoza, J. G. Villegas, "The electric vehicle routing problem with nonlinear charging function," *Transportation Research Part B: Methodological,* In Press, Available online 1 March 2017

[10] F. Milano, and O. Hersent, "Optimal load management with inclusion of electric vehicles and distributed energy resources," *Smart Grid, IEEE Transactions on,* vol. 5pp. 662-672, March 2014.

[11] S. Shafiee, M. Fotuhi-Firuzabad, and M. Rastegar, "Impacts of controlled and uncontrolled PHEV charging on distribution systems," *9th IET International Conference on Advances in Power System Control, Operation and Management*, pp. 1- 6, Sept. 2013.

[12] A. Kavousi-Fard, M. Rostami, T. Niknam, "Reliability-oriented reconfiguration of vehicle-to-grid networks," *Industrial Informatics*, *IEEE Transactions on,* vol. 11, pp. 682-691, 2015.

[13] X. Luo, and K.W. Chan, "Real-time scheduling of electric vehicles charging in low-voltage residential distribution systems to minimise power losses and improve voltage profile," *Generation, Transmission & Distribution, IET,* vol.8, pp.516-529, 2014.

[14] K. Knezovic, Active integration of electric vehicles in the distribution network - theory, modelling and practice, Technical University of Denmark (DTU), PHD thesis, 2017.

[15] L. Cheng, Y. Chang, and R. Huang, "Mitigating voltage problem in distribution system with distributed solar generation using electric vehicles," *Sustainable Energy, IEEE Transactions on,* vol.6, pp.1475-1484, 2015.

[16] A. Kavousi-Fard, T. Niknam, and M. Fotuhi-Firuzabad, "Stochastic reconfiguration and optimal coordination of V2G plug-in electric vehicles considering correlated wind power generation," *Sustainable Energy, IEEE Transactions on,* vol.6, pp.822-830, 2015.

[17] S. Pirouzi, M.A. Latify, and G.R. Yousefi, "Investigation on reactive power support capability of PEVs in distribution network operation," *23rd Iranian Conference on Electrical Engineering (ICEE)*, May 2015.

[18] H. Nafisi, S.M.M. Agah, H. Askarian Abyaneh, and M. Abedi, "Two-stage optimization method for energy loss minimization in microgrid based on smart power management scheme of plug-in hybrid electric vehicles," *Smart Grid, IEEE Transactions on,* vol. 7, pp.11268-1276, 2016.

[19] M.C. Kisacikoglu, M. Kesler, and L.M. Tolbert, "Single-phase on-board bidirectional PEV charger for V2G reactive power operation," *Smart Grid*, *IEEE Transactions on,* vol. 6, pp. 767-775, 2015.

[20] T. Tanaka, T. Sekiya, H. Tanaka, M. Okamoto, and E. Hiraki, "Smart charger for electric vehicles with power-quality compensator on single-phase three-wire distribution feeders," *Industry Applications, IEEE Transactions on,* vol.49, pp.2628-2635, 2013.

[21] L. Yanxia, and J. Jiuchun, "Harmonic-study of electric vehicle chargers," *Proceedings of the Eighth International Conference on Electrical Machines and Systems*. pp. 2404 – 2407, Sept. 2005.

[22] A. Ghosh, and G. Ledwich, Power quality enhancement using custom power devices, *Kluwer Academic Publishers, USA*, 2002.

[23] N.G. Hingorani, and L. Gyugyi, Uderstanding FACTS, *IEEE Press, New York*, 1999.

[24] S. Pirouzi, J. Aghaei, M.A. Latify, G.R. Yousefi, and G. Mokryani, "A robust optimization approach for active and reactive power management in smart distribution networks using electric vehicles," *IEEE System Journal*, (article in press), 2017.

[25] D. Bertsimas, E. Litvinov, X. A. Sun, J. Zhao, and T. Zheng, "Adaptive robust optimization for the security constrained unit commitment problem," *IEEE Trans. Power Syst*., vol. 28, no. 1, pp. 52-63, Feb. 2013.

[26] K.L. Lian, and T. Noda, "Review of harmonic load flow formulations," *Power Delivery*, *IEEE Transactions on,* vol. 18, no. 3, pp. 1079-1087, July 2003.

[27] S. Herraiz, L. Sainz, and J. Clua, "A time-domain harmonic power flow algorithm for obtaining non-sinusoidal steady state solutions," *Power Delivery*, *IEEE Transactions on,* vol. 25, pp. 1888-1899, July 2010.

[28] F.J. Ruiz-Rodriguez, J.C. Hernandez, F. Jurado, "Harmonic modelling of PV systems for probabilistic harmonic load flow studies," *International Journal of Circuit Theory and Applications,* vol. 43, no. 11, pp. 1541-1565, 2015.

[29] S. Pirouzi, J. Aghaei, V. Vahidinasab, T. Niknam and A. Khodaei, "Robust linear architecture for active/reactive power scheduling of EV integrated smart distribution networks," *Electric Power Systems Research*, vol. 155, pp. 8-20, 2017.

[30] H. F. Farahani, H.A. Shayanfar, and M. S. Ghazizadeh, "Modeling of stochastic behavior of PHEV in a reactive power market," *Electric Power Components and Systems*, vol. 96, pp. 31-56, 2012.

[31] J. C. Hernandez, M.J. Ortega, A. Medina, "Statistical characterization of harmonic current emission for large photovoltaic plants," *International Transactions on Electrical Energy Systems*, vol. 24, no. 8, pp. 1134-1150, 2014.

[32] C.K. Duffey, and R. Stratford, "Update of harmonic standard IEEE-519: IEEE recommended practices and requirements for harmonic control in electric power systems," *Industry Applications*, *IEEE Transactions on,* vol. 25, pp. 1025-1034, 1989.

[33] A.J. Wood, and B.F. Wollenberg, Power Generation, Operation and Control, Wiley- Interscience Publication, New york, 1996.

[34] S. Biswas, S. Kumar, and A. Chatterjee, "Optimal distributed generation placement in shunt capacitor compensated distribution systems considering voltage sag and harmonics distortions," *Generation, Transmission & Distribution, IET,* vol.8, pp.783-797, 2014.

[35] A. Kavousi-Fard, and T. Niknam, "Optimal Distribution Feeder Reconfiguration for Reliability Improvement Considering Uncertainty," *Power Delivery, IEEE Transactions on,* vol. 29, pp. 1344-1354, 2014.

[36] Power Systems Test Case Archive, Univ. Washington [Online]. Available: http://www.ee.washington.edu/research/pstca.

[37] R.P. ONeill, A. Castillo, and M.B. Cain, The IV formulation and linear approximations of the AC optimal power flow problem, *FERC Staff Technical Paper*, Dec. 2012.

[38] A.J. Conejo, E. Castillo, R. Minguez, and R. Garcid-Bertrand, Decomposition Techniques in Mathematical Programming, *Springer,* 2006.

[39] J. C. Hernandez, A. Medina, F. Jurado, "Power quality assessment of current electrical vehicle charging processes," *2016 Ieee Pes Asia-Pacific Power and Energy Engineering Conference (APPEEC)*, pp. 1523-1527, 2016.

[40] Generalized Algebraic Modeling Systems (GAMS). [Online]. Available: http://www.gams.com.